Statistics of energy dissipation and stress relaxation in a crumpling network of randomly folded aluminum foils

Alexander S. Balankin,[1] Orlando Susarrey Huerta,[1] and Viktor Tapia[2]
[1]*Grupo "Mecánica Fractal," ESIME-Zacatenco, Instituto Politécnico Nacional, México D.F. 07738, Mexico*
[2]*Universidad Autónoma de Ciudad de México, México D.F. 03020, Mexico*
(Received 1 June 2013; revised manuscript received 31 July 2013; published 5 September 2013)

We study stress relaxation in hand folded aluminum foils subjected to the uniaxial compression force $F(\lambda)$. We found that once the compression ratio is fixed ($\lambda = \text{const}$) the compression force decreases in time as $F \propto F_0 P(t)$, where $P(t)$ is the survival probability time distribution belonging to the domain of attraction of max-stable distribution of the Fréchet type. This finding provides a general physical picture of energy dissipation in the crumpling network of a crushed elastoplastic foil. The difference between energy dissipation statistics in crushed viscoelastic papers and elastoplastic foils is outlined. Specifically, we argue that the dissipation of elastic energy in crushed aluminum foils is ruled by a multiplicative Poisson process governed by the maximum waiting time distribution. The mapping of this process into the problem of transient random walk on a fractal crumpling network is suggested.

DOI: 10.1103/PhysRevE.88.032402 PACS number(s): 46.50.+a, 46.65.+g, 02.50.Ey, 05.40.−a

I. INTRODUCTION

The crumpling of low-dimensional objects displays fascinating features of tremendous importance to both fundamental science and technological applications [1–10]. Crumpling structures arise, for instance, in randomly folded (or crushed) materials ranging from graphene-based nanosheets to geological formations [11–14]. Accordingly, the physics of crumpling and the mechanical properties of randomly folded materials have attracted increasing interest in the last decade (see, for review, Refs. [1–35], and references therein).

In this way, it was recognized that the mechanical response of randomly folded thin matter to an external force is governed by the network of crumpling creases which concentrate the major part of deformation energy [1,5,36]. In an elastic sheet subjected to external confinement the jammed configurations of the crumpling network evolve, leading to rearrangement of energy foci [28,32]. Although a part of the deformation energy can dissipate due to the friction between the crushed sheet surfaces [29,30], the initial (plain) state of an elastic (e.g., rubber) sheet is always restored after the external forces are withdrawn.

In contrast to this, in crushed viscoelastic and elastoplastic sheets a part of the elastic energy is dissipated through irreversible deformations localized in the crumpling creases, as well as due to the friction between sheet surfaces [29,30]. Consequently, under a constant confinement force the specimen size decreases in time due to the elastic strain relaxation caused by irreversible deformations and the collapse of crumpling ridges [4,15,22–24,37]. Furthermore, irreversible deformations create an irretrievable crumpling network providing the permanence of a folded configuration after the external confinement forces are withdrawn [4,8,17].

However, the behavior of crushed viscoelastic and elastoplastic sheets after removing the external confinement forces is quite different. Namely, the release of elastic energy stored in the crumpling creases of viscoelastic paper leads to a slow (logarithmic) increase in the size of the folded sheet over a period of several days, after the external confinement forces are withdrawn [4]. This suggests that the elastic strain relaxation in crushed viscoelastic sheets is ruled by an activated process obeying the Arrhenius-like behavior [22,23]. In contrast to this, the elastic energy stored in the crumpling creases of an aluminum foil is insufficient to change the specimen size or shape by means of elastic strain release [19,24–26]. This indicates that elastic stresses stored in the crumpling creases of elastoplastic aluminum foils are less than the yield stress. Nevertheless, elastic stresses can relax by various deformation mechanisms, such as hillock formation, microstructural changes, and creep, which are characterized by different characteristic time scales (see Ref. [38], and references therein). Specifically, in experiments with thin aluminum films it was found that the stress relaxation can be fitted by the sum of two exponentially decaying terms [39] associated with the fast and slow relaxation processes, respectively [38].

During the uniaxial compression of a folded sheet, a part of the deformation energy is accumulated in the existing crumpling creases, whereas another part is consumed due to the formation of new creases, irreversible deformations, and friction between the sheet surfaces [28,29]. As soon as the uniaxial compression ratio $\lambda = H/R$ (R and H are the specimen size before and after uniaxial compression, respectively) is fixed at a constant level $\lambda_0 = \text{const}$, the compression force F decreases in time due to the rearrangement of energy foci and/or dissipation of elastic energy [22,23,40]. Once again, it is easy to understand that the stress relaxation behavior is dependent on the rheological properties of thin material.

Specifically, in experiments with randomly folded paper balls subjected to the uniaxial compression it was found that at fixed axial confinement $\lambda_0 = \text{const}$ the compression force decreases in time as

$$F = F_0 \left[1 - \beta \ln \left(1 + \frac{t}{\tau_F} \right) \right], \tag{1}$$

where β and τ_F are the material dependent fitting parameters [22,41]. It is pertinent to note that stress relaxation in the paper ball subjected to uniaxial compression ($\lambda_0 = \text{const}$) is

accompanied by a time dependent lateral expansion of the compressed ball. When the compression force is suddenly withdrawn, the compression ratio suddenly increases up to $\lambda_p > \lambda_0$ due to a spontaneous release of a part of the elastic strains and then slowly increases in time as

$$\lambda = \lambda_p \left[1 + c \ln\left(\frac{t}{\tau_r}\right)\right] \tag{2}$$

due to the rest of the elastic strain relaxation over a period of several days, where c and τ_r are fitting constants [42]. It has been argued that the relaxation behavior (1) and (2) can be attributed to activated processes of elastic energy redistribution and dissipation [22].

In contrast to this, in experiments with hand crushed aluminum foils subjected to uniaxial compression, the authors of [40] have observed that the stress decrease at $\lambda_0 = \text{const}$ can be better fitted by the stretched exponential function

$$F = F_0 \exp\left[-\left(\frac{t}{\tau_0}\right)^{\eta}\right], \tag{3}$$

where the fitting parameters η and τ_0 were found to vary in the ranges of $0.24 \leqslant \eta \leqslant 0.4$ and $5 \times 10^3 \leqslant \tau_0 \leqslant 2 \times 10^5$ s, respectively. Moreover, it was conjectured that the scaling exponent $\eta = 0.28 \pm 0.03$ is universal [40]. On the other hand, numerical simulations of stress relaxation on fractal surfaces suggest that the scaling exponent η is dependent on the surface fractal (mass) dimension D [43].

In this context, we noted that the stretched exponential decay (3) is allied with the Weibull distribution of relaxation times [44]. The Weibull distribution emerges from the central limit theorem of extreme value theory as the universal stochastic limit law for distribution of minima of positive valued independent identically distributed random variables [45]. A geometry-based theory for the universal emergence of Weibull distribution was developed in Ref. [46]. Furthermore, the relaxation ruled by the Weibull statistics can be mapped into the problem of random walk on a fractal with the spectral dimension $d_s < 2$ [47,48], such that the scaling exponent η is related to the spectral dimension as

$$\eta = d_s/D < 1, \tag{4}$$

where D is the metric (mass) dimension of the fractal [47]. However, although the Weibull distribution and stretched exponential relaxation are ubiquitous in nature [49–51], we noted that in [40] data fitting with Eq. (3) is rather poor (see Fig. 1 in Ref. [40]) and the range of variations $0.24 \leqslant \eta \leqslant 0.4$ is too large. Accordingly, to understand the stress relaxation in randomly crumpled elastoplastic sheets, in this work we performed a meticulous experimental study with hand folded aluminum foils subjected to uniaxial compression.

II. EXPERIMENTAL FINDINGS

For experimental studies we used aluminum foil of thicknesses $h = 0.06$ mm and mass density $\rho_m = 2.4 \pm 0.1$ g/mm^3 which was earlier exploited in Refs. [19–21]. The stretching yield stress of this foil is $\sigma_{sy} = 15 \pm 5$ MPa and the Young modulus is $Y = 70 \pm 8$ GPa [19,52]. It is pertinent to note that the folding configurations and mechanical properties of randomly crushed aluminum foils were earlier studied in Refs. [7,9,19–21,23–27,53].

A. Experiment details

In this work, the square sheets with edge sizes of L =18, 24, and 30 cm were crushed by hand into spherical balls of an approximate mean diameter R (see Ref. [19]). At least four balls with different compaction ratios $K = L/R$ were folded from sheets of each size. When bending strains exceed the yield point of aluminum foil, this creates a sudden surge of crumpling ridges and vertices. The mean ridge length depends on the sheet size, thickness, and compaction ratio as $\ell = L(h/L)^{\theta} K^{-\alpha}$, where θ and α are the scaling exponents [8], whereas the ridge width is expected [36] to be

$$w = h^{1/3} \ell^{2/3} \ll \ell \ll L \tag{5}$$

for the range of $4 \leqslant K \leqslant 8$ used in this work. We found that Eq. (5) is consistent with the results of experimental estimations of w for ridges located on the surfaces of folded balls.

In the first set of experiments, three balls folded from sheets of different size L were tested under uniaxial loads using a universal test machine MTS-858-5. All experiments were performed with the compression rate of $\dot{H} = dH/dt =$ 6 mm/s (see Fig. 1). Accordingly, in Fig. 2(a) the axial compression force F is plotted versus the compression ratio $\lambda = H/R$. It is pertinent to note that the lateral expansion of the folded aluminum foils subjected to the uniaxial compression was earlier studied in [7]. It was found, that the apparent lateral strain $\varepsilon_{\perp}$ is related to the apparent longitudinal strain $\varepsilon_{||}$ as $\varepsilon_{\perp} = -\nu\varepsilon_{||}$ with the Poisson's ratio $\nu = 0.33 \pm 0.01$ within a wide range of $0 < \varepsilon_{||} \leqslant 0.9$ [7]. This is consistent with experimental observations in the present work.

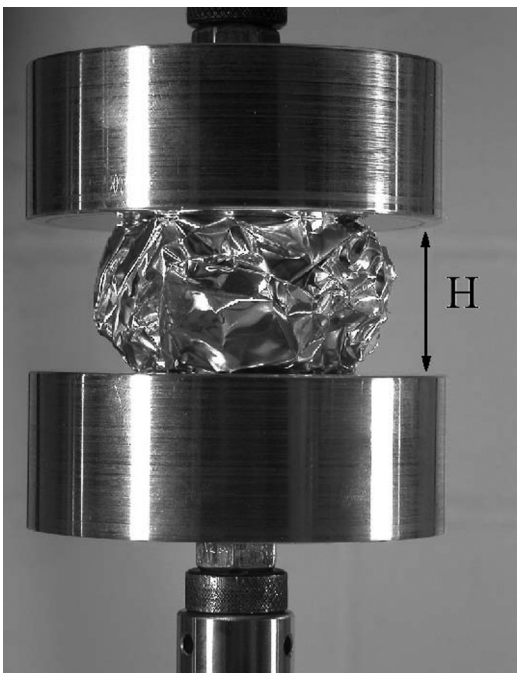

FIG. 1. Setup used to measure the force during the ball compression and relaxation.

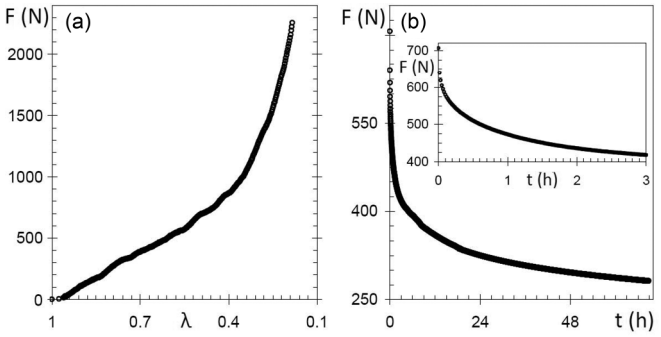

FIG. 2. Typical curves of uniaxial force F in newtons (N) versus (a) dimensionless compression ratio $\lambda = H/R$ for $\dot{H} = 6$ mm/s (L =300 mm; R =50.2 mm) and (b) time t in hours (h) for $\lambda_0 = 0.5$ (L =300 mm; R =49.8 mm). Inset shows the initial part of the relaxation curve.

With the remaining nine balls, the force relaxation tests were performed by suddenly applying a finite amount of constraint $\lambda_0 = H_0/R$ to a specimen and then maintaining it at a constant. While the specimen continues to be "loaded" to the initial constraint $\lambda_0 = \text{const}$, the compression force F drops with time as shown in Fig. 2(b). Furthermore, in three experiments, after several (3, 5, and 8) hours of relaxation the compression force was suddenly removed and possible variations in the specimen height and/or shape were monitored with the help of a laser micrometer MTS LX-500 and a high resolution (6.5 megapixels) video recorder.

B. Force-compression ratio curves

We found that at the loading stage the force-compression curve [see Fig. 2(a)] can be best fitted with the linear relationship

$$F = K_1 \varepsilon_E, \tag{6}$$

where K_1 is the ball stiffness (see Fig. 3), whereas the "effective" relative deformation is defined as

$$\varepsilon_E(t) = (R - H_E)/H_E, \text{ while } H_E = H - nh = R - nh - \dot{H}t, \tag{7}$$

n is the number of layers in the folded ball (see Ref. [22]), and $H(t) = R - \dot{H}t$ is the ball size in the direction of compression [54].

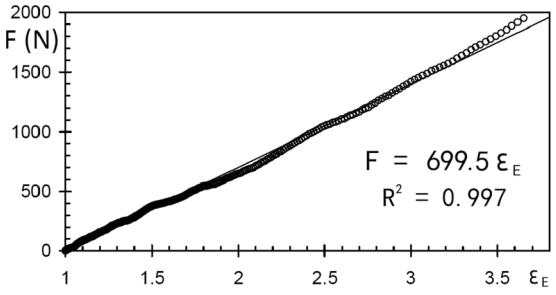

FIG. 3. Typical graphs of the uniaxial force F in newtons versus the dimensionless effective relative deformation ε_E for balls folded from aluminum foils. Symbols: experimental data from Fig. 2(a). Straight lines: data fitting with Eq. (3) .

In this regard, it should be pointed out that in contrast to the scaling behavior $F \propto H^{-\beta}$ with $\beta > 1$ which is observed during the compression of sheets enclosed in a container restricting the radial expansion of crushed sheet (see Refs. [10,15,16,52]), Eqs. (6) and (7) describe the force-compression behavior in experiments with free lateral boundaries of the tested specimen (see Fig. 1).

C. Stress relaxation

Once the compression is stopped at $\lambda_0 = \text{const}$, the compression force decreases in time as shown in Fig. 2(b). First of all, we noted that although the experimental data can be fitted by the stretched exponential function (3), the value of fitting exponent η is dependent on the time interval used for fitting [see Figs. 4(a) and 4(b)]. Specifically, the short-time ($t \ll \tau_0$) asymptotic

$$(1 - \sigma/\sigma_0) \propto t^{\eta_0} \tag{8}$$

is characterized by the scaling exponent η_0 [see inset in Fig. 4(a)] larger than the scaling exponent η found from the fit of the full range data with the stretched exponential function (3), as shown in Fig. 4(a) [55]. Consequently, we have observed systematic deviations from the fitting curve (3) at low and high times [see Fig. 4(b)]. We also noted that although the range of the fitting exponent variation ($0.12 \leqslant \eta \leqslant 0.4$) is consistent with the full experimental range ($0.24 \leqslant \eta \leqslant 0.4$) reported in [40], it contradicts the conjecture of Ref. [40] that $\eta = 0.28 \pm 0.03$ is universal.

At the same time, we found that the best fit to the relaxation behavior in crushed aluminum foils is provided by the following relationship:

$$F = F_0\{1 - \exp[-(\omega t)^{-\gamma}]\}, \tag{9}$$

where the fitting exponent

$$\gamma = 0.14 \pm 0.05 \tag{10}$$

is found to be almost independent on the sheet size L, ball diameter R, and compression ratio λ_0 [see Figs. 4(b) and 5]. In this context, it is also important to note that the value of γ obtained from the long-time ($\omega t \gg 1$) asymptotic behavior

$$F \propto F_0\,(\omega t)^{-\gamma} \tag{11}$$

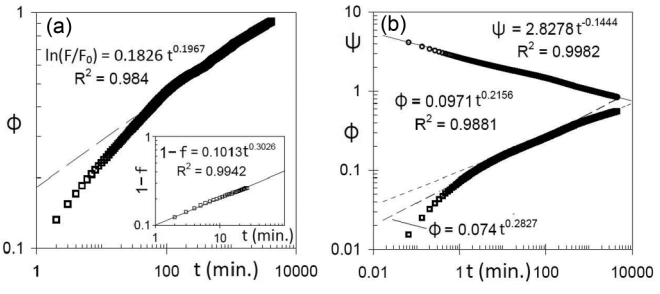

FIG. 4. Typical fittings of force relaxation data: (a) Data from the graph in Fig. 2(b) are fitted with Eq. (2) in log-log coordinates of $\phi = \ln(F/F_0)$ (dimensionless) versus time t (minutes); the inset shows the short-time asymptotic $1 - f \propto t^{\eta}$ in the log-log coordinates ($f = F/F_0$). (b) Log-log plots of dimensionless ϕ (1) and $\psi = \ln(1 - F/F_0)$ (2) versus t in minutes. Straight lines: data fitting with Eqs. (2) and (5), respectively ($L = 240$ mm; $R = 27$ mm; $\lambda_0 = 0.25$).

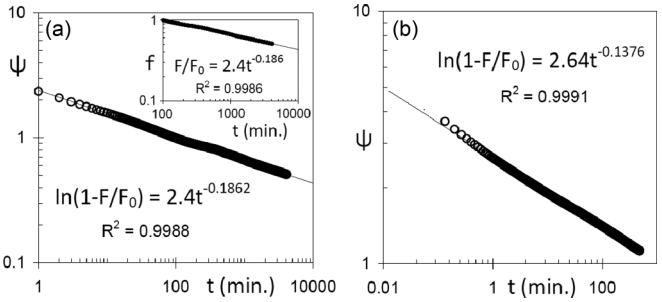

FIG. 5. Log-log plots of dimensionless $\psi = \ln(1 - F/F_0)$ versus t in minutes: (a) data from Fig. 2(b); inset shows the long-time asymptotic $f \propto t^{-\gamma}$. (b) $L = 180$ mm, $R = 22.1$ mm, $\lambda_0 = 0.65$. Symbols: experimental data. Straight lines: data fitting with Eq. (5).

is equal to the value (10) found from the full time range fitting by Eq. (9).

It is pertinent to recall that the stress relaxation behavior in randomly crushed elastoplastic aluminum foils under the uniaxial constraint $\lambda_0 = \text{const}$ differs from stress relaxation (1) observed in experiments with hand folded papers (see Ref. [22]). Furthermore, in experiments when the compression force was suddenly removed at $t > 0$, we have not detected any change in the height of the compressed specimen, in contrast to the logarithmic height increase (2) observed in experiments with hand folded papers (see [42]).

III. DISCUSSION

During the uniaxial compression of a hand folded elastoplastic foil a part of the work of deformation $U(\lambda)$ is lost, whereas the rest is accumulated in the form of elastic energy (E) distributed among the existing and new crumpling creases. Numerical simulations suggest that $E \propto U$ [29,30]. Accordingly, once the compression is suddenly stopped at the moment $t = 0$, the total elastic energy stored in the crumpling network is equal to

$$E(0) = \sum_{i=1}^{N_0} e_i(0) \propto F_0(\lambda_0), \tag{12}$$

where N_0 is the number of crumpling ridges in the crumpling network, while $e_i(t) \geqslant 0$ is the elastic energy stored in the i ridge ($1 \leqslant i \leqslant N_0$) [8,16].

Our observation that there are no changes in the specimen size and shape after the compression force is withdrawn suggests that the elastic stresses in the crumpling creases of elastoplastic foils are less than the yield stress. Nevertheless, at $\lambda_0 = \text{const}$, the elastic energy stored in the crumpling creases dissipates [see Fig. 2(b)] due to stress relaxation caused by processes on the aluminum microstructure level (see Ref. [38]) and friction in the sheet self-contact points (see Refs. [29,30]). Consequently, the compression force decreases in time as

$$F(t) \propto E(t) = \sum_{i=1}^{N(t)} e_i(t), \tag{13}$$

where $N(t) \leqslant N_0$ is the number of ridges storing elastic energy at $t > 0$. Hence, the force decay behavior (9) provides information about the kinetics of energy dissipation in the crumpling network. In this context, the difference between the force decay behavior in randomly crushed viscoelastic papers (1) and elastoplastic aluminum foils (9) suggests that the kinetics of elastic energy dissipation in the crumpling network is dependent on the material rheology.

A. Kinetics of energy dissipation in crumpling network

Let us denote the distribution of elastic energy in the crumpling network at $t = 0$ as $\{e_i(0)\}_0^{N_0}$. At times $t > 0$ the crumpling network undergoes irreversible transitions from the initial state to states with different distributions $\{e_i(t)\}_t^N$. The transition $\{e_i\}_0^{N_0} \to \{e_i\}_t^N$ takes place at a random instant of time τ_i controlled by the waiting and/or relaxation time distributions in the crumpling network. The conditional probability $p(t,dt)$ that the crumpling network will undergo the transition during the time interval $(t,t+dt)$ provided that the transition did not occur before time t can be expressed as $p(t,dt) = \Pr(t \leqslant \tau_i \leqslant t + dt | \tau_i \geqslant t)$. In the limit of $dt \to 0$, the conditional probability is $p(t,dt) = d \ln P(\tau_i \geqslant t)$, where $P(\tau_i \geqslant t)$ is the system's survival probability, that is, the probability that the transition from the initial state did not happen prior to the time instant t. So, the survival probability $P(\tau_i \geqslant t)$ governs the energy dissipation in both time and frequency domains.

It is easy to understand that if the system dynamics is governed by the extreme value statistics, the evolution of elastic energy $E(t > 0)$ should obey the following kinetic equation:

$$\frac{dE}{dt} = E_0 \frac{dP}{dt} = -E_0 f(t), \tag{14}$$

where $f(t) = dP_C/dt$ and $P_C(t) = 1 - P(t)$ are the probability density and cumulative distribution functions, respectively. The explicit form of extreme value distribution function $f(t)$ is determined by statistics of dissipation events.

B. Statistics of energy dissipation in crumpling networks

Generally, the energy dissipation in a crumpling network is controlled by distributions of waiting (τ_{wi}) and/or relaxation (τ_{ri}) times. The former is defined as the time to the event of dissipation, whereas τ_{ri} characterizes the relaxation rate of individual relaxation event $e_i(t) \propto e_{0i} \exp(-t/\tau_{ri})$. Accordingly, the kinetics of energy dissipation is governed by the distribution of minimum relaxation times, if $\tau_{wi} \ll \tau_{ri}$, or by the distribution of maximum waiting times, if $\tau_{wi} \gg \tau_{ri}$.

Specifically, if $\tau_{wi} \ll \tau_{ri}$ and the relaxation times are randomly distributed, the statistics of energy dissipation is controlled by the distribution of minimal relaxation times obeying the Weibull statistics [44]. Accordingly, if the relation (13) holds with $N = \text{const} \gg 1$, from Eq. (14) follows the stretched exponential relaxation behavior (3).

Controversially, if $\tau_{wi} \gg \tau_{ri}$ and the waiting times are randomly distributed, the statistics of energy dissipation is controlled by the distribution of maximum waiting times. According to the central limit theorem of extreme value theory the maximal point of the multiplicative Poisson process is governed by Fréchet statistics [45]. Consequently, if the

relation (13) holds with $N(t) \leqslant N_0$, from Eq. (14) with

$$f(t) = \frac{\gamma}{\omega^{\gamma} t^{\gamma+1}} \exp[-(\omega t)^{-\gamma}] \tag{15}$$

follows the experimentally observed relaxation behavior (9). Notice that Eq. (15) represents the Fréchet probability density distribution function, where $\gamma > 0$ is the scaling exponent and ω^{-1} plays the role of time scale. Accordingly, Eq. (14) can be rewritten in the form

$$\frac{dE}{dt} = \frac{\gamma E_0}{t}\left(1 - \frac{E}{E_0}\right) \ln\left(1 - \frac{E}{E_0}\right), \tag{16}$$

which does not explicitly include the time scale. Notice that no systematic dependence of ω on L, R, or λ_0 was observed in our experiments. Thus, the relaxation behavior (9) suggests that the energy dissipation in the crumpling network of an elastoplastic crushed aluminum foil is governed by the waiting time distribution belonging to the domain of attraction of the max-stable distribution of the Fréchet type.

In contrast to this, in the case of $\tau_{wi} \approx \tau_{ri}$ the energy dissipation is not expected to obey any extreme value statistics. Therefore, in this case the elastic energy evolution should not obey Eq. (14). Specifically, in Ref. [22] it has been argued that the stress relaxation in crushed viscoelastic paper (1) is governed by the activated processes of elastic energy redistribution and dissipation.

C. Model of energy dissipation in crumpling network with $\tau_{wi} \gg \tau_{ri}$

Although the Fréchet distribution is one of the three extreme value distributions [44], to the best of our knowledge, the relaxation behavior of type (9) was never reported in the literature. Nonetheless, the simplest model leading to Eq. (9) can be formulated as follows. At $t = 0$ the elastic energy stored in the crumpling network with N_n ridges is randomly distributed among $N_0 \leqslant N_n$ ridges. Following the ideas of Ref. [56], the dissipation of elastic energy can be treated as a Poisson process defined for $t > 0$ and characterized by two random variables: the waiting times $\{\tau_{wi}\}_t^N$ and the dissipation rates (or durations) $\{\tau_{ri}\}_t^N$. If $\tau_{ri} \ll \tau_{wi}$, the number of ridges conserving the elastic energy at $t > 1$ is equal to $N(t) = N_0[1 - P_C(t)]$, whereas the rest of the $N_0 P_C(t)$ ridges are in the state with $e_i \cong 0$. Therefore, the total energy stored in the crumpling network is expected to behave as

$$E(t) = \sum_{i}^{N(t)} e_i(0) \propto E_0 \frac{N(t)}{N_0} = E_0 [1 - P_C(t)], \tag{17}$$

where $P_C(t)$ is the cumulative distribution of maximum waiting times obeying the Fréchet statistics.

Consequently, taking into account relationship (13), the force relaxation behavior (9) is immediately followed from Eq. (17). Furthermore, the force relaxation in the frequency domain can be obtained in a straightforward way (see [51]) by taking the one-sided Fourier transform of waiting time probability density function (15).

Although our experiments do not provide information about mechanisms of energy dissipation in a crumpling crease of crushed aluminum foil, the relaxation behavior (9) suggests that the relaxation times (durations) of consecutive dissipation events are much less than the waiting times between them, that is, $\tau_{wi} \gg \tau_{ri}$. So, one can speculate that the elastic energy dissipation in crushed aluminum foils under the constraint $\lambda_0 = \text{const}$ can be ruled by the sudden jumps in the points of sheet self-contact which are controlled by the friction phenomena. Furthermore, the elastic energy stored in a crumpling crease can dissipate by the short range diffusion mechanisms, such as Coble and Nabarro-Herring creep (see Ref. [38], and references therein) with the relaxation time (of around 5 min [38]) much less than the characteristic waiting time (of the order of 1 h).

D. Mapping of energy dissipation processes into processes of random walks on fractal crumpling networks

It is a straightforward matter to expect that the distribution of waiting times $\{\tau_{wi}\}_t^N$ in the crushed thin sheets is controlled by the scaling properties of fractal crumpling networks storing the major part of elastic energy. Hence, the Poisson process of elastic energy dissipation can be mapped into a random walk on a fractal crumpling network (to this respect, see Refs. [47,48]).

The dynamics of random walk on a fractal network is governed by the network spectral dimension $d_s = 2D/D_W$, where D is the fractal dimension (e.g., mass, self-similarity, or Hausdorff dimension) of the network and D_W is the random walk dimension [57–59]. If $d_s < 2$, then $D_W > D$ and the random walk is recurrent, whereas if $d_s > 2$, then $D_W < D$ and so the random walk is transient [58]. Therefore, the number of sites (ridges) unvisited by a random walker on the fractal crumpling network of fixed size N_n exhibits the power-law asymptotic decay

$$N \propto t^{-(d_s-2)/2}, \tag{18}$$

if the spectral dimension of crumpling network $d_s > 2$ [60]. If relations (13) and (17) hold, from Eqs. (11) and (18) it follows that the scaling exponent γ is related to the spectral dimension of the crumpling network as

$$\gamma = d_s/2 - 1 > 0, \tag{19}$$

as long as $d_s > 2$. Hence, the independence of scaling exponent (10) of the L, K, and λ_0 suggests that the spectral dimension of crumpling networks in randomly crushed aluminum foils

$$d_s = 2(1 + \gamma) = 2.3 \pm 0.1 \tag{20}$$

is independent of geometric constraints, but it can be material dependent. Specifically, we noted that the value (20) differs from the spectral dimension of crumpling network $d_s = 1.53 \pm 0.06 < 2$ which was found in experiments with a hand crushed paper (see Ref. [8]). Although a specific reason for this difference is unclear, it may be attributed to different rheology of viscoelastic paper and elastoplastic aluminum foils. Consequently, the statistics of elastic energy dissipation appear to be different for crumpling networks with $d_s < 2$ ($\tau_{wi} \approx \tau_{ri}$) and $d_s > 2$ ($\tau_{wi} \gg \tau_{ri}$), respectively.

IV. CONCLUSIONS

Summarizing, we found that under a sufficiently fast uniaxial compression a randomly folded aluminum foil displays linear force-effective relative deformation behavior (6). As

soon as the compression ratio is fixed, the decrease of uniaxial compression force exhibits rather unconventional time behavior (9). We argue that this finding suggests that the dissipation of elastic energy in a crumpling network can be considered as a fractal Poisson process with the Fréchet distribution of maximum waiting times. Furthermore, we suggest that the energy dissipation process can be mapped into the problem of transient random walk on the fractal crumpling network with the spectral dimension $d_s > 2$. The difference between the elastic energy dissipation statistics in the crumpling networks of randomly crushed viscoelastic papers ($d_s < 2$) and elastoplastic aluminum foils ($d_s > 2$) is outlined.

In this regard, it is pertinent to point out that our arguments are rather generic and should hold at the nanoscale [61], as well as at the geological scales [62]. So, our findings offer a general insight into the physics of crumpling and provide a framework to understand the relaxation processes in randomly folded matter of different nature.

ACKNOWLEDGMENTS

This work was supported by the PEMEX under the research SENER-CONACYT Grant No. 143927.

[1] T. A. Witten, Rev. Mod. Phys. **79**, 643 (2007).
[2] J. A. Astrom, J. Timonen, and M. Karttunen, Phys. Rev. Lett. **93**, 244301 (2004); D. L. Blair and A. Kudrolli, *ibid.* **94**, 166107 (2005); E. Sultan and A. Boudaoud, *ibid.* **96**, 136103 (2006); P. M. Reis, F. Corson, A. Boudaoud, and B. Roman, *ibid.* **103**, 045501 (2009); D. P. Holmes and A. J. Crosby, *ibid.* **105**, 038303 (2010); J. Hure, B. Roman, and J. Bico, *ibid.* **109**, 054302 (2012).
[3] T. Tallinen, J. Ojajärvi, J. A. Aström, and J. Timonen, Phys. Rev. Lett. **105**, 066102 (2010); R. D. Schroll, E. Katifori, and B. Davidovitch, *ibid.* **106**, 074301 (2011); H. Diamant and T. A. Witten, *ibid.* **107**, 164302 (2011); B. Roman and A. Pocheau, *ibid.* **108**, 074301 (2012); S. S. Datta, S.-H. Kim, J. Paulose, A. Abbaspourrad, D. R. Nelson, and D. A. Weitz, *ibid.* **109**, 134302 (2012).
[4] A. S. Balankin, O. Susarrey, R. Cortes, D. Samayoa, J. Martínez, and M. A. Mendoza, Phys. Rev. E **74**, 061602 (2006).
[5] A. S. Balankin, R. Cortes, and D. Samayoa, Phys. Rev. E **76**, 032101 (2007); A. S. Balankin, D. Samayoa, I. A. Miguel, J. Patiño, and M. A. Martínez Cruz, *ibid.* **81**, 061126 (2010).
[6] A. S. Balankin and O. Susarrey, Phys. Rev. E **77**, 051124 (2008).
[7] A. S. Balankin, D. Samayoa, E. Pineda, R. Cortes, A. Horta, and M. A. Martínez Cruz, Phys. Rev. B **77**, 125421 (2008).
[8] A. S. Balankin, A. Horta, G. García, F. Gayosso, H. Sanchez, and C. L. Martínez-González, Phys. Rev. E **87**, 052806 (2013).
[9] G. Seizilles, E. Bayart, M. Adda-Bedia, and A. Boudaoud, Phys. Rev. E **84**, 065602(R) (2011).
[10] S. Deboeuf, E. Katzav, A. Boudaoud, D. Bonn, and M. Adda-Bedia, Phys. Rev. Lett. **110**, 104301 (2013).
[11] J. Zhang, J. Xiao, X. Meng, C. Monroe, Y. Huang, and J.-M. Zuo, Phys. Rev. Lett. **104**, 166805 (2010); K. Kim, Z. Lee, B. D. Malone, K. T. Chan, B. Alemán, W. Regan, W. Gannett, M. F. Crommie, M. L. Cohen, and A. Zettl, Phys. Rev. B **83**, 245433 (2011); J. Luo, H. D. Jang, T. Sun, L. Xiao, Z. He, A. P. Katsoulidis, M. G. Kanatzidis, J. Murray Gibson, and J. Huang, ACS Nano **5**, 8943 (2011); J. Agbenyega, Mater. Today **14**, 578 (2011); P. M. Reis, Nat. Mater. **10**, 907 (2011); N. B. Le and L. M. Woods, Phys. Rev. B **85**, 035403 (2012); C. N. Lau, W. Bao, and J. Velasco, Jr., Mater. Today **15**, 238 (2012); J. Zang, S. Ryu, N. Pugno, Q. Wang, Q. Tu, M. J. Buehler, and X. Zhao, Nat. Mater. **12**, 321 (2013).
[12] S. W. Cranford and M. J. Buehler, Phys. Rev. B **84**, 205451 (2011).
[13] X. Ma, M. R. Zachariah, and C. D. Zangmeister, Nano Lett. **12**, 486 (2012); W.-N. Wang, Y. Jiang, and P. Biswas, J. Phys. Chem. Lett. **3**, 3228 (2012).
[14] N. Cardozo, R. W. Allmendinger, and J. K. Morgan, J. Struct. Geol. **27**, 1954 (2005); D. M. Hansen and J. Cartwright, *ibid.* **28**, 1520 (2006); Z. Ismat, *ibid.* **31**, 972 (2009); B. E. Hobbs, A. Ord, and K. Regenauer-Lieb, *ibid.* **33**, 758 (2011).
[15] K. Matan, R. B. Williams, T. A. Witten, and S. R. Nagel, Phys. Rev. Lett. **88**, 076101 (2002).
[16] G. A. Vliegenthart and G. Gompper, Nat. Mater. **5**, 216 (2006).
[17] C. A. Andresen, A. Hansen, and J. Schmittbuhl, Phys. Rev. E **76**, 026108 (2007).
[18] R. Cassia-Moura and M. A. F. Gomes, J. Theor. Biol. **238**, 331 (2006).
[19] A. S. Balankin, I. Campos, O. A. Martínez, and O. Susarrey, Phys. Rev. E **75**, 051117 (2007).
[20] A. S. Balankin, D. Morales, E. Pineda, A. Horta, M. Á. Martínez, and D. Samayoa, Physica A **388**, 1780 (2009).
[21] A. S. Balankin, S. Matías, D. Samayoa, J. Patiño, B. E. Elizarraraz, and C. L. Martínez-González, Phys. Rev. E **83**, 036310 (2011).
[22] A. S. Balankin, O. Susarrey, F. Hernández, and J. Patiño, Phys. Rev. E **84**, 021118 (2011).
[23] I. I. Dierking and P. P. Archer, Phys. Rev. E **77**, 051608 (2008).
[24] Y. C. Lin, Y. L. Wang, Y. Liu, and T. M. Hong, Phys. Rev. Lett. **101**, 125504 (2008).
[25] Y. C. Lin, J. M. Sun, J. H. Hsiao, Y. Hwu, C. L. Wang, and T. M. Hong, Phys. Rev. Lett. **103**, 263902 (2009).
[26] Y. C. Lin, J. M. Sun, H. W. Yang, Y. Hwu, C. L. Wang, and T. M. Hong, Phys. Rev. E **80**, 066114 (2009).
[27] W. Bai, Y. C. Lin, T. K. Hou, and T. M. Hong, Phys. Rev. E **82**, 066112 (2010).
[28] T. Tallinen, J. A. Aström, and J. Timonen, Phys. Rev. Lett. **101**, 106101 (2008).
[29] T. Tallinen, J. A. Aström, and J. Timonen, Nat. Mater. **8**, 25 (2009).
[30] T. Tallinen, J. A. Aström, and J. Timonen, Comput. Phys. Commun. **180**, 512 (2009).
[31] T. Tallinen, J. A. Aström, P. Kekäläinen, and J. Timonen, Phys. Rev. Lett. **105**, 026103 (2010).
[32] H. Aharoni and E. Sharon, Nat. Mater. **9**, 993 (2010).

[33] R. S. Mendes, L. C. Malacarne, R. P. B. Santos, H. V. Ribeiro, and S. Picoli, Jr., Europhys. Lett. **92**, 29001 (2010).
[34] A. B. Thiria and M. Adda-Bedia, Phys. Rev. Lett. **107**, 025506 (2011).
[35] M. A. F. Gomes, C. C. S. Pereira, and V. P. Brito, Phys. Rev. E **87**, 052103 (2013).
[36] A. Lobkovsky, S. Gentges, H. Li, D. Morse, and T. A. Witten, Science **270**, 1482 (1995); E. M. Kramer and T. A. Witten, Phys. Rev. Lett. **78**, 1303 (1997); G. Gompper, Nature (London) **386**, 439 (1997); B. A. DiDonna and T. A. Witten, Phys. Rev. Lett. **87**, 206105 (2001); B. A. DiDonna, T. A. Witten, S. C. Venkataramani, and E. M. Kramer, Phys. Rev. E **65**, 016603 (2001); B. A. DiDonna, *ibid*. **66**, 016601 (2002); M. M. Muller, M. Ben Amar, and J. Guven, Phys. Rev. Lett. **101**, 156104 (2008); T. Liang, Phys. Rev. E **77**, 056602 (2008); J. W. Wang and T. A. Witten, *ibid*. **80**, 046610 (2009).
[37] In experiments with polymer films crumpled under a constant compressive force it was observed that the long-term stress relaxation is superimposed by discontinuous stress jumps which were attributed to sudden collapses of crumpling ridges [23].
[38] S.-J. Hwang, Y.-D. Lee, Y.-B. Park, J.-H. Lee, C.-O. Jeong, and Y.-C. Joo, Scr. Mater. **54**, 1841 (2006).
[39] In contrast to logarithmic decay of bending stresses observed in experiments with single folded paper sheets [34].
[40] R. F. Albuquerque and M. A. F. Gomes, Physica A **310**, 377 (2002).
[41] Logarithmic decay of bending stresses was also observed in experiments with polymer films [23].
[42] A. S. Balankin and O. S. Huerta, in *Proceedings of the IUTAM Symposium on Scaling in Solid Mechanics*, edited by F. M. Borodich (Springer, London, 2009), pp. 233–241.
[43] K. P. Mota and P. M. C. de Oliveira, Physica A **387**, 6095 (2008).
[44] I. Eliazar and R. Metzler, Phys. Rev. E **87**, 022141 (2013).
[45] I. Eliazar and J. Klafter, Phys. Rev. E **82**, 021122 (2010).
[46] I. Eliazar, Phys. Rev. E **86**, 031103 (2012).
[47] P. Jund, R. Jullien, and I. Campbell, Phys. Rev. E **63**, 036131 (2001).
[48] M. Kozlowska and R. Kutner, Physica A **357**, 282 (2005).
[49] *Non-Debye Relaxation in Condensed Matter*, edited by T. V. Ramakrishnan and L. Raj Lakshmi (World Scientific, Singapore, 1987); J. C. Phillips, Rep. Prog. Phys. **59**, 1133 (1996); B. Dodson, *The Weibull Analysis Handbook* (ASQ Press, Milwaukee, 2006); J. I. McCool, *Using the Weibull Distribution: Reliability, Modeling and Inference* (Wiley, New York, 2012).
[50] I. Eliazar and I. M. Sokolov, Phys. Rev. E **81**, 011122 (2010); I. Eliazar and J. Klafter, *ibid*. **82**, 011112 (2010); Phys. Rep. **511**, 143 (2012).
[51] R. Hilfer, Phys. Rev. E **65**, 061510 (2002).
[52] O. Bouaziz, J. P. Masse, S. Allain, L. Orgéas, and P. Latil, Mater. Sci. Eng. A **570**, 1 (2013).
[53] M. A. F. Gomes, T. I. Jyh, T. I. Ren, I. M. Rodrigues, and C. B. S. Furtado, J. Phys. D: Appl. Phys. **22**, 1217 (1989).
[54] It is pertinent to note that at lower deformation rates we have observed deviations from Eq. (6), which can be attributed to energy dissipation during the ball compression.
[55] This feature can also be observed in Fig. 1 of Ref. [40]. So, there is no contradiction between experimental data reported in [40] and that obtained in the present work.
[56] I. Eliazar and J. Klafter, Phys. Rev. E **77**, 061125 (2008); Physica A **387**, 4985 (2008); I. Eliazar, Eur. Phys. J. Spec. Top. **216**, 3 (2013).
[57] U. Mosco, Phys. Rev. Lett. **79**, 4067 (1997).
[58] S. Halvin and D. Ben-Avraham, Adv. Phys. **51**, 187 (2002).
[59] A. S. Balankin, B. Mena, C. L. Martínez-González, and D. M. Matamoros, Phys. Rev. E **86**, 052101 (2012).
[60] If $d_s < 2$ the random walk is recurrent and so all sites (ridges) in a fractal crumpling network of finite size will be visited by random walker within a finite time interval.
[61] In this context, it is pertinent to note that the similarity between the geometry and mechanics of random crumpling of aluminum foils and graphene-based structures was pointed out in Ref. [13].
[62] It is worth noting the remarkable similarities between earthquakes and the intermittent acoustic noise emitted by crumpled plastic sheets pointed out in [33]. In this context, the statistical framework suggested in this paper can be used to model the aftershock sequence that follows an earthquake.